PHYSICAL REVIEW B VOLUME 3, NUMBER 6 15 MARCH 1971

Phonon Coupling and Angular Dispersion in Biaxial $NaNO_2$†

C. M. Hartwig, E. Wiener-Avnear, J. Smit, and S. P. S. Porto
Departments of Physics and Electrical Engineering, University of Southern California, Los Angeles, California 90007
(Received 3 August 1970)

A detailed Raman investigation of the angular dispersion of the five phonons, propagating in oblique directions in the *ac* plane of biaxial $NaNO_2$, is reported. It is shown that this dispersion is caused by the coupling of all the vibrational modes through the induced longitudinal electric field. When the polarization configurations used in the Raman measurements are along the principal axes of the crystal, all the coupled modes are then detectable, leading to apparent selection-rule violations. For two dimensions the analysis yields a frequency-gap picture, which accounts quantitatively for the experimental results. An expression for the Raman intensities of the oblique phonons is also given.

Recent Raman experiments upon oblique phonons (polar phonons which are propagating at oblique angles to their ionic polarizations) have shown curious phenomena.[1-3] In biaxial $NaNO_2$, oblique phonon spectra have revealed[1,2] more lines in a particular polarization configuration than are predicted by the standard group-theory analysis for the fundamental modes. Furthermore, the frequencies of these phonons have shown unexplained angular dispersion. In another investigation, the oblique-phonon angular dispersion[3] of uniaxial $LiIO_3$ has been shown to fit the Loudon approximation,[4] determined by the assumption of anisotropy dominance over the long-range electrostatic field, even when the inequality of frequencies that necessitates this assumption was not satisfied. As a part of a general survey of the connection between the ferroelectric properties and the lattice dynamics of $NaNO_2$,[5] we had to measure LO frequencies, using a near-forward Raman scattering experiment. We then encountered similar anomalies; more lines appeared than were expected, and they showed shifted frequencies that were neither the pure LO nor TO values. We were thus motivated to survey the behavior of the oblique phonons in this biaxial crystal. This paper presents a detailed investigation of the angular dispersion and mode coupling of the five B_1 and B_2 Raman-active polar modes, traveling in the *ac* plane of $NaNO_2$. A classical macroscopic model, based upon the coupling of any number of modes presented by the long-range induced electric field, is developed and shown to describe the experiments. This analysis is applicable to crystals of orthorhombic or higher symmetry.

At room temperature, $NaNO_2$ is orthorhombic with space-group symmetry C_{2v}^{20} (one molecule per primitive cell). Group theory allows the following irreducible modes[5]:

$$3A_1(aa, bb, cc): b + 1A_2(ac) + 3B_1(bc): c + 2B_2(ab): a \ ,$$

where a, b, and c refer to conventional designations of the biaxial-crystal's axes.[6] The Raman activities are put in parentheses. The polarization direction of each mode is indicated in the letter following the bracket.

Raman scattering from a zero-degree cut $NaNO_2$ single crystal has been applied to detect the oblique phonons.[5] By controlling the incident light beam direction, different oblique phonons could be selected for observation. The following scattering geometries, which allow the detection of B_1 and B_2 phonons propagating in the *ac* crystallographic plane, were used: $(xc+ya)(ba)c$, $(xc+ya)(ba)a$, and $(xc+ya)(a+c, b)a$ (x, y are arbitrary). The scattering-tensor components (bc) and (ba) used in the experiment may be regarded as filters that select either B_1 or B_2 phonons, respectively. The behavior of A_1 and A_2 phonons is not reported, because it adds no additional insight to the oblique-phonon clarification. The angle ϕ, which will be used to parametrize the angular dispersion, is the angle between the direction of the phonon propagation in the *ac* plane and the *c* axis.

Figures 1(a)–1(f) present some of the anomalous Raman spectra that we observed in the external-mode region. In Figs. 1(a) and 1(d), two resonances are seen, which correspond to pure fundamental TO modes of B_1 and B_2 character, as is expected for transversal scattering configurations with (ab) and (bc) polarization filters, respectively. In Figs. 1(b) and 1(c), and Figs. 1(e) and 1(f), which show the spectral results of some oblique phonons, four, or sometimes three, resonances with unidentified frequencies are observed with the (ab) and (bc) polarization filters. The additional lines are apparent violations of selection rules based upon standard group-theory analysis for the fundamentals of the B_1 and B_2 modes, and are not due to crystal misorientation, crystal birefringence, or to the finite solid angle of the gathering lens. The angular dispersion values of the three B_1 and two B_2 oblique modes, traveling in the *ac* plane, are given in Fig.

2, which also denotes the different polarization filters and scattering geometries used.

In Fig. 2 the highest frequency-angular curve describes the internal B_1 oblique phonons. It shows a clean sweep between the TO and LO values without the appearance of additional lines nearby. The behavior of the four lower frequency-dispersion curves describing the external modes is more complicated and exhibits the following phenomena:

(i) In certain angular regions the same eigenfrequency can be observed with different polarization filters, indicating a mixing of modes of different symmetries.

(ii) There seems to be no simple *a priori* designation of the pairs of end points between which the angular-dispersion curves are continuously scanning. The following pairings occur in $NaNO_2$: $B_2(TO) \rightarrow B_1(TO)$; $B_1(LO) \rightarrow B_1(TO)$; $B_2(TO) \rightarrow B_2(LO)$; and $B_1(LO) \rightarrow B_2(LO)$. The assignments of the various modes in Fig. 2 have been established by temperature studies.[5]

(iii) At no angles do any of the angular-dispersion curves cross. Therefore, frequency gaps appear along the energy ordinate in which no phonon propagation occurs.

(iv) The frequency values of all the dispersion curves in Fig. 2 are either monotonically increasing or decreasing.

Raman experiments select phonons whose wave-vector magnitudes q are of the order of light; therefore, the dipolar interaction can be represented by an induced macroscopic electric field $\vec{E}$. Since the wave vectors do not reach into the polariton region, $q^2c^2/\omega^2 \gg \epsilon_0$, the electrostatic approximation holds

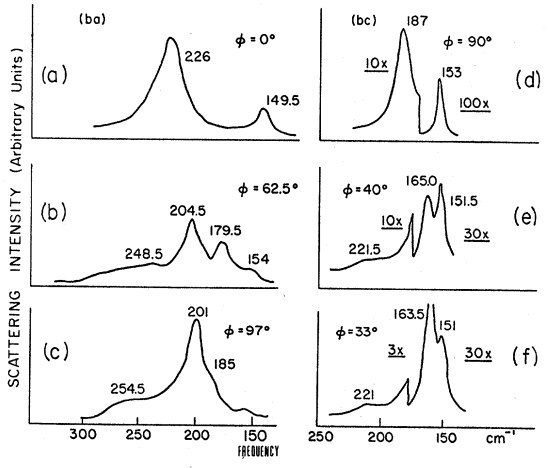

FIG. 1. Raman spectra of oblique phonons in $NaNO_2$. (a)–(c) are spectra seen through the (*ba*) polarization filter, and (d)–(f) are spectra seen through the (*bc*) filter. The angle ϕ is measured between $\vec{q}$ and the c axis on the ac plane. Resonant frequencies (in cm^{-1}) and scale changes are indicated.

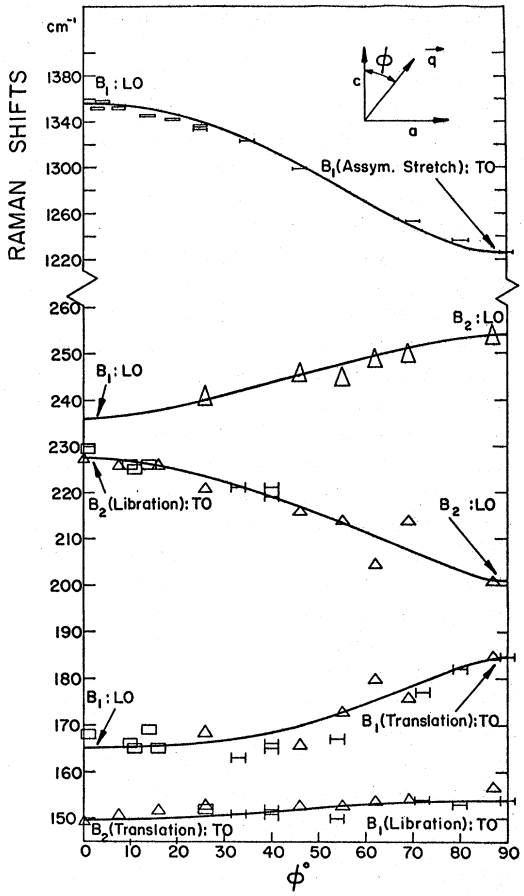

FIG. 2. Oblique-phonon angular dispersion in $NaNO_2$. The triangles (△) are data points taken with the (*bc*) polarization filter; the bars (⊢⊣) refer to the (*ba*) filter, and the boxes (□) refer to the ($a+c$, b) filter. The endpoint characters of the various branches are marked on the graph.

($\vec{\nabla} \times \vec{E} = 0$), restricting the electric field to being parallel to the phonon-propagation direction ($E_\perp = 0$). In an insulator, $\vec{\nabla} \cdot \vec{D} = 0$; therefore, $D_\parallel \cong \epsilon_\parallel E_\parallel = 0$, or

$$\epsilon_\parallel = \sum_m \sum_k \alpha_m \alpha_k \epsilon_{mk} = 0 , \qquad (1)$$

where α_k are the direction cosines of $\vec{q}$. For crystals with orthorhombic symmetry or higher, there exists a unique set of principal axes for the dielectric constant. Ignoring damping mechanisms,[7] the oblique-phonon frequency $\omega_{\vec{q}}$ can be found from

$$\epsilon_\parallel = \sum_k \alpha_k^2 \epsilon_{\infty k} \prod_{i=1}^{N_k} \frac{\omega_{ik}^2(\mathrm{LO}) - \omega_{\vec{q}}^2}{\omega_{ik}^2 - \omega_{\vec{q}}^2} = 0 , \qquad (2)$$

where the product extends over the N_k LO frequencies $\omega_{ik}(\mathrm{LO})$ and the TO fundamental frequencies ω_{ik} with polarizations along the k axis. Equation (2) can also be derived from previous work by Merten.[8] Restricting the oblique-phonon propagation to a major plane, denoted as ac to relate to our $NaNO_2$ experiments, (2) can be reduced to an ex-

plicit expression for the angular dispersion:

$$\tan^2\phi = -\frac{\epsilon_{\infty c}}{\epsilon_{\infty a}} \prod_{i=1}^{N_a} \prod_{j=1}^{N_c} \frac{(\omega_{ia}^2 - \omega_\phi^2)(\omega_{jc}^2(\mathrm{LO}) - \omega_\phi^2)}{(\omega_{jc}^2 - \omega_\phi^2)(\omega_{ia}^2(\mathrm{LO}) - \omega_\phi^2)} , \quad (3)$$

where ϕ is defined as above. Inspection shows that any angular-dispersion curve ω_ϕ that satisfies (3) has the properties stated in the experimental observations (ii), (iii), and (iv).

The theoretical angular-dispersion curves (3) for $NaNO_2$ ($N_a = 2$; $N_c = 3$) are plotted in Fig. 2, showing an excellent fit with the experimental values. The five observed TO frequencies[5] for B_1 and B_2 used in (3) correspond well with previous measurements.[6,9] The LO frequency values are not accurately known[5,6,9] and were treated as adjustable parameters in order to achieve the best fit with the experimental points throughout the angular range. Thus, the oblique-phonon frequency-dispersion study provides a more accurate method to determine the LO values, which is especially important for cases where the Raman scattering intensity of the LO mode tends to diminish. The resulting TO and LO frequencies of B_1 and B_2 modes are denoted in Fig. 2.

At any angle ϕ, the oblique phonon of branch j is a mixture of the fundamental modes. In the classical limit, we expect the amplitude of the oblique-phonon Raman scattered wave, seen through a polarization filter which selects fundamental modes polarized parallel to axis k, to be linear in the amplitudes of the ionic polarizations P_{ik} of the fundamental modes:

$$I_{j\vec{q},k} = 2\pi[\textstyle\sum_i (A_{ik}/S_{ik}^{1/2}) P_{ik}(\omega_{j\vec{q}}) + B_k E_k/4\pi]^2 . \quad (4)$$

B_k is related to the electro-optical coefficient, and the dielectric transition strength S_{ik} is given by

$$S_{ik} = \epsilon_{\infty k} \textstyle\prod_j [\omega_{jk}^2(\mathrm{LO}) - \omega_{ik}^2]/\omega_{ik}^2 \prod_{j\neq i} (\omega_{jk}^2 - \omega_{ik}^2) . \quad (5)$$

The factors A_{ik} can be found experimentally (up to a sign) from the intensities of the Stokes lines at the fundamental TO modes,

$$I_{ik}(\mathrm{TO}) = A_{ik}^2 (\bar{n}_{ik} + 1)\hbar\omega_{ik} ,$$

where $\bar{n}_{ik}$ is the thermal population factor for frequency ω_{ik}. For arbitrary $\vec{q}$,

$$I_{j\vec{q},k} = \frac{\alpha_k^2 \left(\sum_{i=1}^{N_k} \frac{A_{ik} S_{ik}^{1/2} \omega_{ik}^2}{(\omega_{ik}^2 - \omega_{j\vec{q}}^2)} + B_k \right)^2}{\sum_m \alpha_m^2 \sum_{i=1}^{N_m} \frac{S_{im} \omega_{j\vec{q}}^2 \omega_{im}^2}{(\omega_{im}^2 - \omega_{j\vec{q}}^2)^2}} (\bar{n}_{j\vec{q}} + 1)\hbar\omega_{j\vec{q}} . \quad (6)$$

There is qualitative agreement between (6) and our experimental results.

In conclusion, the problem of multioblique phonons confined to propagate in a plane is easily interpreted by the previous analysis, giving a gap-frequency-type picture. For a noninteracting mode, the oblique phonon will scan between its pure TO and LO frequencies. In case of frequency-overlapping modes, which electrostatically interact, the destinations of the angular-dispersion curves can be predicted by (3) and will depend only on the relative positioning of the pure TO and LO frequencies of all the modes involved. The previous ideas of dominancy of electric field over anisotropy or vice versa[4,10,11] to describe the angular-dispersion behavior are only special cases, which are usually not applicable to the general oblique-phonon behavior. Indeed, better agreement was obtained between the experimental angular-dispersion results of uniaxial $LiIO_3$[3] and the predictions of (3) than with the earlier theory. Also, the relative intensities, observed by a polarization filter, of the TO and LO frequencies in cubic $NaClO_3$ for oblique propagation[12] conform to (6). The general analysis described above is, therefore, a very powerful tool for investigating the oblique-phonon behavior in cubic uniaxial and biaxial crystals of orthorhombic symmetries.

†Work supported by the National Science Foundation under Grant No. 19109 and the Joint Services Electronics Program (U. S. Army, U. S. Navy, and U. S. Air Force) under Grant No. AFOSR-69-1622.

[1]C. K. Asawa and M. K. Barnoski, Phys. Rev. B (to be published).

[2]M. Tsuboi, M. Terada, and T. Kjiura, Bull. Chem. Soc. Japan 42, 1871 (1969).

[3]W. Otaguro, C. A. Arguello, and S. P. S. Porto, Phys. Rev. B 1, 2818 (1970).

[4]R. Loudon, in *Proceedings of the International Conference on Light Scattering Spectra of Solids, New York*, 1968 (Springer, New York, 1969), p. 25.

[5]C. M. Hartwig, E. Wiener-Avnear, and S. P. S. Porto (unpublished).

[6]M. K. Barnoski and J. M. Ballantyne, Phys. Rev. 174, 946 (1968).

[7]The damping mechanism can be accounted for by applying the formula suggested by A. S. Barker, Phys. 136, A1290 (1964).

[8]L. Merten, Z. Naturforsch. 229, 359 (1967); Phys. Status Solidi 25, 125 (1968).

[9]J. D. Axe, Phys. Rev. 167, 573 (1968).

[10]H. Poulet, Ann. Phys. (Paris) 10, 908 (1955).

[11]C. A. Arguello, D. L. Rousseau, and S. P. S. Porto, Phys. Rev. 181, 1351 (1969).

[12]C. M. Hartwig, D. L. Rousseau, and S. P. S. Porto, Phys. Rev. 188, 1328 (1969).